Supplementary Information (SI) for Materials Advances.

Unlocking the Full Potential of Solar Cell Materials: Parameter Sensitivity Analysis and Optimization Using Response Surface Modelling

Manoj Kumar[1*], Sanju Rani[2], Xu Wang[3*], Vidya Nand Singh[4*]

[1]School of Basic and Applied Science, IILM University, Knowledge Park-II, Greater Noida, Uttar Pradesh- 201306

[2]Department of Electrical Engineering, Indian Institute of Technology Mandi, Kamand, Himachal Pradesh 175075, India

[3]School of Engineering, RMIT University Victoria 3001, Australia

[4]Indian Reference Materials (BND) Division, CSIR-National Physical Laboratory, Dr. K. S. Krishnan Marg, New Delhi-110012, India

Table S1. Input parameters/variables for the device

Parameter	**SnSe**	**TiO_2** [1]	**SnO_2**
Thickness (µm)	**1.2**	**0.10**	**0.2**
Band gap (eV)	**1-1.5** [2]	**2.26**	**3.6** [3]
Electron Affinity (eV)	**4.2** [2], [4]	**4.1-4.5**	**4.53** [3]
Valence band density of states (cm^{-3})	**1.6 $x10^{18}$**	**6 $x10^{17}$**	**1 $x10^{19}$** [5]
Conduction band density of states (cm^{-3})	**1.45 $x10^{18}$**	**2 $x10^{17}$**	**1 $x10^{19}$** [6]
Radiative recombination coefficient (cm^3s^{-1})	**2.9 $x10^{-11}$**	**1 $x10^{-8}$**	**1 $x10^{-8}$**
Mobility of electron/hole (cm^2/Vs)	**130/56.7** [7]	**100/50**	**5/2.5** [6]
Absorption coefficient	**5 $x10^4$** [2]	**-**	**-**
Uniform Acceptor density (cm^{-3})	**$9x10^{15}$- $4x10^{16}$**	**-**	**-**
Uniform donor density (cm^{-3})	**-**	**$1x10^{17}$**	**$1x10^{19}$** [5]

Band gap of the TiO_2 is taken as 2.26 (which can be easily obtained after doping[8], [9]**.**

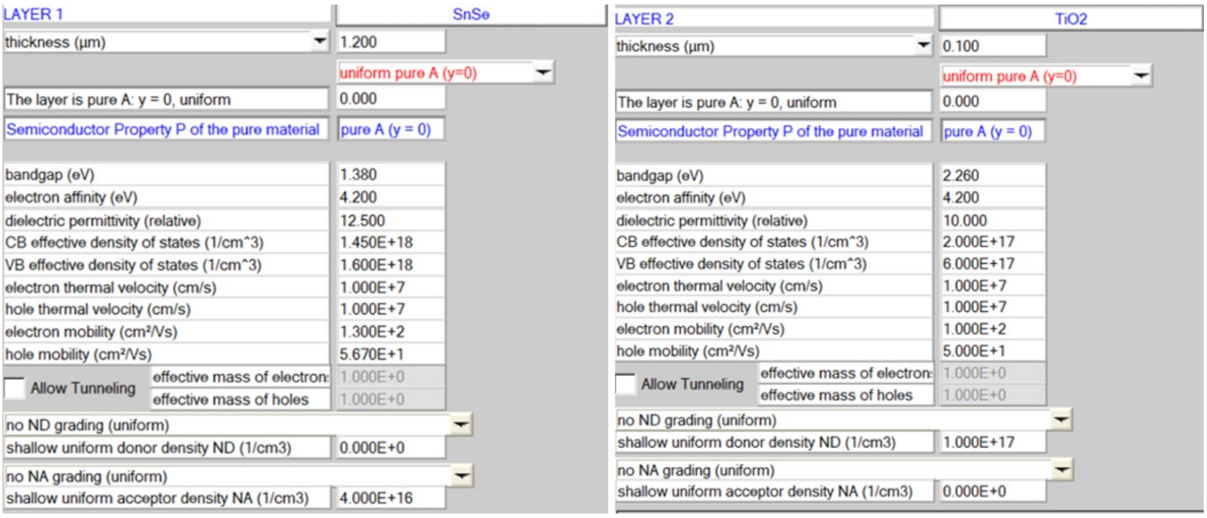

Figure S1 The input parameters for the SnSe (left) and for TiO_2 (right) in SCAPS-1D.

Table S2. Set of parameters (z_i) (with 5 variables, face-centered alpha =1.56508) using central composite design (CCD).

Sr. No.	Z_1	Z_2	Z_3	Z_4	Z_5
1	-1	-1	-1	-1	-1
2	1	-1	-1	-1	-1
3	-1	1	-1	-1	-1
4	1	1	-1	-1	-1
5	-1	-1	1	-1	-1
6	1	-1	1	-1	-1
7	-1	1	1	-1	-1
8	1	1	1	-1	-1
9	-1	-1	-1	1	-1
10	1	-1	-1	1	-1
11	-1	1	-1	1	-1
12	1	1	-1	1	-1
13	-1	-1	1	1	-1
14	1	-1	1	1	-1
15	-1	1	1	1	-1
16	1	1	1	1	-1
17	-1	-1	-1	-1	1
18	1	-1	-1	-1	1
19	-1	1	-1	-1	1
20	1	1	-1	-1	1
21	-1	-1	1	-1	1
22	1	-1	1	-1	1
23	-1	1	1	-1	1
24	1	1	1	-1	1

25	-1	-1	-1	1	1
26	1	-1	-1	1	1
27	-1	1	-1	1	1
28	1	1	-1	1	1
29	-1	-1	1	1	1
30	1	-1	1	1	1
31	-1	1	1	1	1
32	1	1	1	1	1
33	-1.56058	0	0	0	0
34	1.56058	0	0	0	0
35	0	-1.56058	0	0	0
36	0	1.56058	0	0	0
37	0	0	-1.56058	0	0
38	0	0	1.56058	0	0
39	0	0	0	-1.56058	0
40	0	0	0	1.56058	0
41	0	0	0	0	-1.56058
42	0	0	0	0	1.56058
43	0	0	0	0	0
44	0	0	0	0	0
45	0	0	0	0	0
46	0	0	0	0	0
47	0	0	0	0	0
48	0	0	0	0	0
49	0	0	0	0	0
50	0	0	0	0	0

Table S3 Input parameters using the CCD for the simulation and their efficiency after simulation by SCAPS-1D

Sr. No.	Band Gap (x_1)	Shallow Acceptor Density (x_2)	CBO(x_3)	W.F. (x_4)	Temp. (x_5)	Efficiency (R)
	eV	1/cm^3	eV	eV	K	%
1	1	9 x10^{+15}	-0.1	4.8	275	15.77
2	1.5	9x10^{+15}	-0.1	4.8	275	9.02
3	1	4x10^{+16}	-0.1	4.8	275	17.12
4	1.5	4x10^{+16}	-0.1	4.8	275	9.84
5	1	9x10^{+15}	0.3	4.8	275	16.54
6	1.5	9x10^{+15}	0.3	4.8	275	9.17
7	1	4x10^{+16}	0.3	4.8	275	18.21
8	1.5	4x10^{+16}	0.3	4.8	275	10.23

9	1	$9x10^{+15}$	-0.1	5.4	275	27.31
10	1.5	$9x10^{+15}$	-0.1	5.4	275	19.97
11	1	$4x10^{+16}$	-0.1	5.4	275	27.3
12	1.5	$4x10^{+16}$	-0.1	5.4	275	19.98
13	1	$9x10^{+15}$	0.3	5.4	275	29.95
14	1.5	$9x10^{+15}$	0.3	5.4	275	19.47
15	1	$4x10^{+16}$	0.3	5.4	275	29.95
16	1.5	$4x10^{+16}$	0.3	5.4	275	20.01
17	1	$9x10^{+15}$	-0.1	4.8	320	14.99
18	1.5	$9x10^{+15}$	-0.1	4.8	320	9.23
19	1	$4x10^{+16}$	-0.1	4.8	320	16.22
20	1.5	$4x10^{+16}$	-0.1	4.8	320	10.18
21	1	$9x10^{+15}$	0.3	4.8	320	14.68
22	1.5	$9x10^{+15}$	0.3	4.8	320	8.85
23	1	$4x10^{+16}$	0.3	4.8	320	16.1
24	1.5	$4x10^{+16}$	0.3	4.8	320	9.98
25	1	$9x10^{+15}$	-0.1	5.4	320	26.44
26	1.5	$9x10^{+15}$	-0.1	5.4	320	18.8
27	1	$4x10^{+16}$	-0.1	5.4	320	26.44
28	1.5	$4x10^{+16}$	-0.1	5.4	320	18.85
29	1	$9x10^{+15}$	0.3	5.4	320	27.18
30	1.5	$9x10^{+15}$	0.3	5.4	320	17.94
31	1	$4x10^{+16}$	0.3	5.4	320	27.18
32	1.5	$4x10^{+16}$	0.3	5.4	320	18.42
33	0.85873	$2.45x10^{+16}$	0.1	5.1	297.5	23.09
34	1.64127	$2.45x10^{+16}$	0.1	5.1	297.5	13.26
35	1.25	$2.4126x10^{+14}$	0.1	5.1	297.5	16.16
36	1.25	$4.87587x10^{+16}$	0.1	5.1	297.5	20.21
37	1.25	$2.45x10^{+16}$	-0.213	5.1	297.5	16.7
38	1.25	$2.45x10^{+16}$	0.413	5.1	297.5	17.82
39	1.25	$2.45x10^{+16}$	0.1	4.63048	297.5	9.31
40	1.25	$2.45x10^{+16}$	0.1	5.56952	297.5	29.94
41	1.25	$2.45x10^{+16}$	0.1	5.1	262.286	21.69
42	1.25	$2.45x10^{+16}$	0.1	5.1	332.714	18.1
43	1.25	$2.45x10^{+16}$	0.1	5.1	297.5	19.98
44	1.25	$2.45x10^{+16}$	0.1	5.1	297.5	19.98
45	1.25	$2.45x10^{+16}$	0.1	5.1	297.5	19.98
46	1.25	$2.45x10^{+16}$	0.1	5.1	297.5	19.98
47	1.25	$2.45x10^{+16}$	0.1	5.1	297.5	19.98
48	1.25	$2.45x10^{+16}$	0.1	5.1	297.5	19.98
49	1.25	$2.45x10^{+16}$	0.1	5.1	297.5	19.98
50	1.25	$2.45x10^{+16}$	0.1	5.1	297.5	19.98

Tablx10 S4. Actual value of the efficiency from SCAPS-1D software and the predicted value of the efficiency by RSM model and their Residual.

Run Order	Actual Value of Efficiency	Predicted Value of Efficiency	Residual
1	18.10	18.84	-0.7404
2	9.98	9.36	0.6159
3	19.98	19.86	0.1225
4	18.21	18.26	-0.0487
5	9.84	10.38	-0.5394
6	27.30	28.02	-0.7165
7	10.18	10.05	0.1303
8	16.10	15.99	0.1110
9	18.80	19.09	-0.2909
10	19.98	19.86	0.1225
11	9.23	8.59	0.6389
12	10.23	10.70	-0.4688
13	23.09	24.51	-1.42
14	9.02	8.92	0.0992
15	15.77	15.23	0.5392
16	16.22	15.42	0.7954
17	29.94	28.40	1.54
18	16.54	16.80	-0.2602
19	19.98	19.81	0.1709
20	9.17	9.24	-0.0702
21	13.26	12.91	0.3522
22	19.98	19.86	0.1225
23	16.70	17.45	-0.7504

24	19.98	19.86	0.1225
25	16.16	18.00	-1.84
26	20.01	20.13	-0.1185
27	27.31	27.63	-0.3180
28	20.21	19.44	0.7661
29	14.99	13.97	1.02
30	17.12	16.69	0.4307
31	21.69	20.87	0.8155
32	26.44	26.75	-0.3118
33	19.47	19.74	-0.2700
34	18.85	19.48	-0.6294
35	8.85	7.91	0.9444
36	19.98	19.86	0.1225
37	29.95	29.59	0.3641
38	14.68	14.53	0.1495
39	19.98	19.86	0.1225
40	19.97	19.42	0.5495
41	17.94	18.41	-0.4653
42	27.18	27.32	-0.1362
43	27.18	26.93	0.2523
44	9.31	11.32	-2.01
45	17.82	18.14	-0.3220
46	19.98	19.86	0.1225
47	26.44	26.36	0.0767
48	19.98	19.86	0.1225
49	29.95	29.20	0.7526
50	18.42	18.79	-0.3738

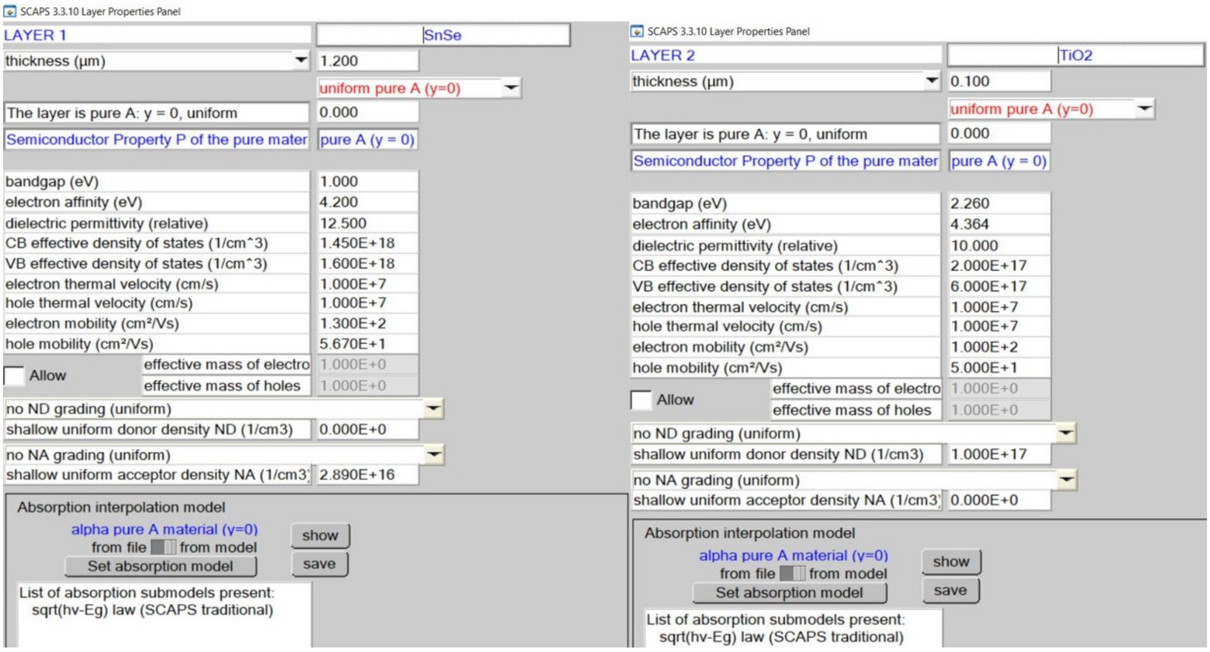

Figure S2. Input panel for the (left) SnSe, and (right) TiO_2.

References

[1] W. Ahmad, A. D. Khan, and W. Ahmad, "Design and Simulation of High-Efficiency Two-Dimensional Carbon Nitride Design and Simulation of High-Efficiency Two-Dimensional Carbon Nitride (C 2 N-h2D) Solar Cell with SnS (HTL) and TiO 2 (ETL) via SCAPS-1D," in *Proceedings of the 4th International Conference on Sustainable Energy Technologies (ICSET 2022) Peshawar, Pakistan*, 2022, vol. 2, no. December. doi: 10.5281/zenodo.8047694.

[2] M. Kumar, S. Rani, Y. Singh, A. Kumar, and V. N. Singh, "Strategy to improve the efficiency of tin selenide based solar cell : A path from 1.02 to 27.72%," *Sol. Energy*, vol. 232, no. November 2021, pp. 146–153, 2022, doi: 10.1016/j.solener.2021.12.069.

[3] M. U. Hajiev and R. R. Kabulov, "Features of w-sn02/p-si structural heteroj unction manufactured by the chemical steam-gas deposition method," *Int. J. Thin Film Sci. Technol.*, vol. 10, no. 2, pp. 83–87, 2021, doi: 10.18576/ijtfst/100202.

[4] M. Kumar *et al.*, "Large area, self-powered, flexible, fast, and broadband photodetector enabled by the SnSe-Sb2Se3 heterostructure," *Surfaces and Interfaces*, vol. 30, no. April, p. 101964, 2022, doi: 10.1016/j.surfin.2022.101964.

[5] R. A. Rassol, R. F. Hasan, and S. M. Ahmed, "Numerical analysis of SnO2/Zn2SnO4/n-CdS/p-CdTe solar cell using the SCAPS-1D simulation software," *Iraqi J. Sci.*, vol. 62, no. 2, pp. 505–516, 2021, doi: 10.24996/ijs.2021.62.2.17.

[6] B. A. D. Williamson *et al.*, "Resonant Ta Doping for Enhanced Mobility in Transparent Conducting SnO2," *Chem. Mater.*, vol. 32, no. 5, pp. 1964–1973, 2020, doi: 10.1021/acs.chemmater.9b04845.

[7] R. K. Yadav *et al.*, "A qualitative study of SnSe thin film solar cells using SCAPS 1D and comparison with experimental results: A pathway towards 22.69% efficiency," *Sol. Energy*

Mater. Sol. Cells, vol. 244, no. May, p. 111835, 2022, doi: 10.1016/j.solmat.2022.111835.

[8] W. Li *et al.*, "Band gap tailoring of Nd3+-doped TiO2 nanoparticles," *Appl. Phys. Lett.*, vol. 83, no. 20, pp. 4143–4145, 2003, doi: 10.1063/1.1627962.

[9] V. A. Mu'izayanti and H. Sutrisno, "Structural and optical properties of AgCl-sensitized TiO2 (TiO2@AgCl) prepared by a reflux technique under alkaline condition," *Ceramica*, vol. 64, no. 370, pp. 190–196, 2018, doi: 10.1590/0366-69132018643702311.